Article:
Scalabrin, M, Engman, V, Maccannell, A et al. (2022) Temporal analysis of skeletal muscle remodelling post hindlimb ischemia reveals intricate autophagy regulation. American Journal of Physiology: Cell Physiology, 323 (6). C1601-C1610. ISSN: 0363-6143

https://doi.org/10.1152/ajpcell.00174.2022

Temporal analysis of skeletal muscle remodelling post hindlimb ischemia reveals intricate autophagy regulation

Mattia Scalabrin[1], Viktor Engman[1], Amanda Maccannell[2], Annabel Critchlow[1], Lee D. Roberts[2], Nadira Yudalsheva[2], T. Scott Bowen[1]

1. School of Biomedical Science, Faculty of Biological Science, University of Leeds, UK.
2. Leeds Institute of Cardiovascular and Metabolic Medicine, University of Leeds, UK

Short title: skeletal muscle remodelling following ischemia

Supplementary materials are available at:
DOI: https://doi.org/10.6084/m9.figshare.20472237

Corresponding author:

T. Scott Bowen, PhD

School of Biomedical Sciences,

Faculty of Biological Sciences,

University of Leeds, Leeds,

United Kingdom,

LS2 9JT

Tel: (+44) 113 343 3834

Email: t.s.bowen@leeds.ac.uk

Abstract

Hind Limb Ischemia (HLI) is the most severe form of peripheral arterial disease, associated with a substantial reduction of limb blood flow that impairs skeletal muscle homeostasis to promote functional disability. The molecular regulators of HLI-induced muscle perturbations remain poorly defined. This study investigated whether changes in the molecular catabolic-autophagy signalling network were linked to temporal remodelling of skeletal muscle in HLI.

HLI was induced via hindlimb ischemia (femoral artery ligation) and confirmed by Doppler echocardiography. Experiments were terminated at time points defined as early- (7 days; n=5) or late (28 days; n=5) stage HLI. Ischemic and non-ischemic (contralateral) limb muscles were compared. Ischemic vs. non-ischemic muscles demonstrated overt remodelling at early-HLI but normalised at late-HLI. Early-onset fibre atrophy was associated with excessive autophagy signalling in ischemic muscle: protein expression increased for Beclin-1, LC3 and p62 ($p<0.05$) but proteasome-dependent markers were reduced ($p<0.05$). Mitophagy signalling increased in early-stage HLI which aligned with an early and sustained loss of mitochondrial content ($p<0.05$). Upstream autophagy regulators Sestrins showed divergent responses during early-stage HLI (Sestrin2 increased while Sestrin1 decreased; $p<0.05$) in parallel to increased AMPK phosphorylation ($p<0.05$) and lower antioxidant enzyme expression. No changes were found in markers for mTORC1 signalling.

These data indicate early-activation of the sestrin-AMPK signalling axis may regulate autophagy to stimulate rapid and overt muscle atrophy in HLI, which is normalised within weeks and accompanied by recovery of muscle mass. A complex interplay between Sestrins to regulate autophagy signalling during early-to-late muscle remodelling in HLI is likely.

Key words: Ischemia, Skeletal Muscle, Autophagy, Sestrins

Abbreviations

4EBP1	Eukaryotic translation initiation factor 4E-binding protein 1
AMPK	AMP-activated protein kinase
CSA	Cross Sectional Area
CuZnSOD	Superoxide Dismutase 1
Drp1	Dynamin-like Protein 1
GC	Gastrocnemius
HLI	Hind Limb Ischemia
HO-1	Heme-oxygenase 1
LC3	Microtubule-associated Protein 1A/1B-Light Chain 3
Mfn2	Mitofusin 2
MnSOD	Superoxide Dismutase 2
mTORC1	Mechanistic target of rapamycin complex 1
MuRF1	Muscle RING-Finger protein-1
Nrf-2	Nuclear factor-erythroid factor 2-related factor 2
OPA1	Optic Atrophy 1 protein
rbS6	Ribosomal protein S6
UPS	Ubiquitin Proteasome System

Introduction

Hind Limb Ischemia (HLI) is the most severe form of peripheral vascular disease in humans, affecting over 200 million people worldwide (1-3). HLI reduces lower limb blood flow to cause symptoms of pain and disability, with limb amputation and death also reported (2, 3). A major outcome in HLI patients is severely reduced functional mobility, which worsens within 6 months of diagnosis (4, 5). The underlying mechanisms that contribute towards functional decline in HLI patients are poorly established. Impairments to skeletal muscle homeostasis are strongly implicated, which may include changes related to loss of innervation (6), fibre atrophy, contractile dysfunction, increased ectopic fat deposition and mitochondrial derangements (4). However, there remains a paucity of data explaining what molecular events contribute towards this temporal and functional decline in muscle subjected to HLI.

HLI is associated with early-onset muscle wasting, which is closely linked with functional disability (7). Muscle mass is controlled by a complex interplay between anabolic and catabolic signalling pathways (8), with macro-autophagy (herein referred to as autophagy) a major catabolic component (9). Autophagy is vital for maintaining cellular homeostasis (10) given its role in delivering dysfunctional proteins and organelles to the autolysosome for degradation (11). However, perturbed regulation leading to sustained increases or decreases in autophagy results in overt muscle pathology (9). Previous studies using different models of HLI including cerebral ischemia (12), ischemia/reperfusion (13) and femoral occlusion (14-16) implicate autophagy as a central mechanism in the muscle wasting process. Noteworthy, autophagy seems to be upregulated early (i.e. within 2 hours post-ischemic injury (15)) but evidence indicates that despite driving atrophy, this activation may promote muscle survival and revascularization (16). Hence, autophagy could be critical for normal muscle regeneration and physiological recovery in HLI.

Autophagy is regulated by a network complicated mirage of upstream signalling mechanisms (17). Among these, a family of newly discovered small stress-induced proteins called Sestrins have been suggested as potential master regulators of skeletal muscle homeostasis and autophagy (18). The Sestrin family contains three

proteins (Sestrin 1-3) (19), with Sestrin 1 and Sestrin 2 being the two isoforms mainly expressed in skeletal muscle (20). Recent evidence further suggest that Sestrins, whose levels decrease in several muscle atrophy conditions and ageing, play a central role as mediators of the beneficial effects of exercise training by protecting skeletal muscle homeostasis (i.e. by regulating autophagy through AMP-activated protein kinase (AMPK) (13, 20)) but also by regulating regeneration via effects on muscle stem cells (21). In addition, Sestrins either directly (via their oxidoreductase activity) or indirectly (via activation of the Nuclear factor-erythroid factor 2-related factor 2 (Nrf2) signalling pathway) modulate oxidative stress in muscle and accumulation of oxidative damage (22).

Overall whether progressive muscle remodelling following HLI is linked to temporal changes in autophagy signalling is poorly defined (23-26). This study explored the autophagy signalling axis during skeletal muscle remodelling in severe ischemia. Targeting autophagy regulation may offer novel therapeutic targets for patients with HLI.

Materials and Methods

Animal procedures

Twelve weeks old C57BL/6 male mice (n=10) were included in this study and provided ad libitum access to standard chow and water. Experiments were performed under UK Home Office animal guidelines (Scientific Procedures) Act 1986 and received ethical approval from the University of Leeds Animal Welfare Ethical Review Body. The number of mice per group (n=5) was based upon past studies (16, 23, 24, 27) which showed they were powered to detect differences in our primary measure of muscle mass. Mice underwent unilateral surgery to induce HLI in the left lower hindlimb, with the right limb serving as control (i.e. non ischemia). Prior to surgery, mice were anesthetized with a mix of Isoflurane 0.2% and O_2 and alongside received an injection of buprenorphine (analgesic; 1mg/kg sc). The femoral artery and vein were isolated, ligated and then fully dissected to induce ischemia while preventing collateralization, as previously detailed (24, 28, 29). After surgery, the external wound was sutured and mice were maintained in warmed cages until recovery. Mice were sacrificed via cervical dislocation at 7 days (n=5) and 28 days (n=5) and dissected skeletal muscles were weighed then immediately snap frozen in liquid nitrogen and stored at -80^{o}C until further analysis, whereas the soleus was prepared for histological analysis as below.

Laser Doppler Flowmetry

Laser Doppler Flowmetry was performed on Moor LDI2-HR (Moor Systems, UK) before, 7 days and 28 days after surgery (23). Briefly, mice were anesthetized with a mix of isoflurane 0.2%, placed on a heated map and kept under anaesthesia throughout the entire duration of the recording. Images were collected and analysed using a MoorLDI software, Version 5.3 (Moor Systems, UK) by comparing the ischemic to non-ischemic limb perfusion ratio, based upon flux below the level of the inguinal ligament.

SDS-PAGE western blot

The gastrocnemius (GC) muscles from the left and right limbs were ground in liquid nitrogen and the resulting powder added to 200µl of RIPA buffer (Merk, Darmstadt, Germany) with the addition of Pierce™ Protease and Phosphatase Inhibitor Mini

Tablets, EDTA Free (Thermo Fisher Scientific, Waltham, MA, USA). SDS-PAGE and immunoblotting analysis were performed as previously described (30). Ponceau red (Sigma-Aldrich Ltd, Gillingham, Dorset, United Kingdom) was used to verify the effectiveness of transfer procedure and GADPH (Cell Signalling Technology, Danvers, MA, USA) used as a housekeeping protein to normalize the results. Primary antibodies were detected using recommended HRP-linked secondary antibodies (Cell Signalling Technology, Danvers, MA, USA; see supplementary material Table 1) and Chemiluminescent signal was detected using the G.Box imaging system (Syngene, Cambridge, UK) following addition of ECL (Thermo Fisher Scientific, Waltham, MA, USA). Analysis of densitometry was performed using ImageJ software, as previously described (30). A representative image of the protein ladder (Thermo Fisher Scientific, Waltham, MA, USA) used to determine the molecular weights during the experiments is presented in Supplementary Figure 1.

Immunohistochemical analysis

Soleus muscles were mounted directly on a cork disk, surrounded with O.C.T. mounting medium (Thermo Fisher Scientific, Waltham, MA,USA), frozen rapidly in isopentane cooled in liquid nitrogen and sectioned (12µm) using a cryostat (Leica CM1850, Leica, Wetzlar, Germany) as previously described (31). To assess fibre cross-sectional area (CSA) and fibre type distribution, sections were re-hydrated and blocked for 1 hour in 5% Goat Serum (Thermo Fisher Scientific, Waltham, MA, USA) + M.O.M. Blocking (Vector Lab, Burlingame, CAL, USA). Sections were then incubated for 60 minutes with BA-D5 (IgG2B, 1:250 - MyHCI fibres) and SC-71 (IgG1,1:250 - MyHCIIa fibres) (Developmental Studies Hybridoma Bank, Iowa City, IA, USA) and respective secondary antibodies (conjugated goat anti-mouse IgG2b, 1:500 - Thermo Fisher Scientific, Waltham, MA). Muscle fibre boundaries were labelled using Wheat Germ Agglutinin, Rhodamine (1:1000; Vector Lab, Burlingame, CAL, USA). Slides were then imaged at magnifications of x20 using the Zeiss Axioscan Z1 slides scanner (Zeiss AG, Jena, Germany). Sections were analysed using Myovision (University of Kentucky) and ImageJ software. To stain for fibres boundaries and nuclei localisation, sections were fixed with 100% ice-cold methanol and then incubated for 10 minutes in Wheat Germ Agglutinin, Rhodamine (1:1000; Vector Lab, Burlingame, CAL, USA). Slides were then mounted using a mounting

media with DAPI (Vector Lab, Burlingame, CAL, USA) and visualised on a Zeiss Axioscan Z1 slides scanner (Zeiss AG, Jena, Germany).

Citrate synthase assay

The citrate synthase assay was performed using a previously published protocol (32). Briefly, GC muscles were cryopulverised and resulting powder added to 200µl of RIPA buffer (Merk, Darmstadt, Germany) with the addition of Pierce™ Protease and Phosphatase Inhibitor Mini Tablets, EDTA Free (Thermo Fisher Scientific, Waltham, MA, USA). Samples were sonicated 3 times for 15 sec and centrifuged at 12,000g for 10 min at 4ºC. Supernatant was collected and protein content quantified using the BCA assay. Citrate synthase activity was measured by detecting the transfer of sulfhydryl groups to 5,5′-dithiobis (2-nitrobenzoic acid) (DTNB) at a wavelength of 412nm with readings performed every 20 seconds for a total of 6 minutes using a PowerWave HT plate reader (BioTek, Vermont, Canada). Before performing the assay, 1µl of sample were added to the plate reader together with 199µl of the reaction solution (100 mM Tris · HCl, 0.2 mM acetyl CoA, 0.1 mM DTNB; pH 8.1) and incubated for 5 minutes at 37°C. Following incubation, an endpoint reading of the background signal was performed before adding 10µl of Oxaloacetate (10mM) to begin the experiment. Each sample was run in triplicate, means normalised to protein content and calculated as µmol/min/mg; data are presented as percentage of control.

Statistical Analysis

Statistical analysis was performed using IBM SPSS statistic version 22 software (IBM analytics, New York, USA). All tests were carried out with a 95% confidence interval and the level of significance was set at 0.05. Normal distribution was checked using the Shapiro-Wilk test while the Levene's test was used to verify the Equality of Variance in our groups. Data was expressed as the mean ± standard error mean (SEM). Independent sample two-tailed t-test was used to detect differences between the control and the ischemic groups, unless otherwise noted. When the normality of distribution assumption was not met, the Mann-Whitney U test was used. Outliers were detected using the established ROUT statistical method (33) and the recommended Q (maximum desired False Discovery Rate) of 1%, with the final sample size for each experiment noted in each figure legend.

240

Results

Limb blood flow and muscle remodelling post ischemia

HLI was confirmed by analysing pre- and post-limb perfusion in the control vs. ligated limb (Figure 1a). At 7 days post-surgery, the mean blood flux in the lower hind limb was impaired vs. contralateral limb by (-73%; $U(8)= -2.611$, $p<0.05$; Figure 1b). However, perfusion was increased at 28 days post-surgery by one third (-44%; $p>0.05$; Figure 1c) indicative of partial revascularization of the lower hindlimb. Despite limited total body mass change (Fig. 1d, e), 7 days of HLI resulted in loss of muscle wet-mass vs. contralateral limb (both GC and soleus; $p<0.05$; Figure 1f, h). Histological evidence reinforced this finding, with soleus fibre cross-sectional area showing atrophy at 7 days ($t(8)=2.51$, $p<0.05$; Figure 2a-b) alongside altered fibre composition (i.e. shift from type I to type IIa $p<0.05$; Figure 2c). In contrast, at 28 days post HLI wet-mass in GC muscle increased vs control ($t(5.6)=-3.243$, $p<0.05$; Figure 1g), despite no differences in soleus wet-mass, fibre cross-sectional area or composition ($p>0.05$; Figure 2d-f). Interestingly, soleus showed reappearance of type I fibres towards control levels and a robust regenerative potential at 28 days, as demonstrated by increased fibres with centralised nuclei (+68%) in ischemic muscle that was in general absent in contralateral ($t(8)=-5.731$; $p<0.05$; Figure 2g-h).

Catabolic signalling via autophagy is activated at early HLI stages

Given the finding of early-onset muscle wasting after 7 days HLI, we first explored key catabolic signalling pathways. To monitor the progression of autophagy signalling following ischemia-induced fibre atrophy, several markers were investigated in the GC muscle. Beclin-1 protein content, a reliable marker of autophagy initiation (34), was increased by 6 fold vs. contralateral muscle ($t(8)=4.943$, $p<0.05$; Figure 3a) but normalised to control levels at 28 days ($p>0.05$; Figure 3b). A similar trend was found with microtubule-associated protein 1A/1B-light chain 3 (LC3), a reliable marker of autophagosome formation (34), with increased protein content of both LC3-I ($t(8)=14.133$, $p<0.05$; Figure 3c) and LC3-II ($t(8)=1.965$, $p<0.05$; Figure 3e) after 7 days in ischemic vs. contralateral muscle with a similar trend seen in the ratio of these two proteins which did not reach statistical significance ($p>0.05$; figure 3 i). However at 28 days, protein content of LC3-I and LC-II and their ratio were normalised in ischemic muscle to contralateral control values ($p>0.05$; Figure 3d, f, l). Supporting the hypothesis of increased activation of

autophagy at early but not late stages of HLI; protein expression of p62 (SQSTM1) was decreased in ischemic vs. control muscle at 7 days ($t(8)=1.632$, $p<0.05$; Figure 3g) but normalised at 28 days ($p>0.05$; Figure 3h). In addition to autophagy, a major pathway mediating muscle wasting is the ubiquitin proteasome system (UPS) which is regulated in part by increased expression of key E3 ligases (termed atrogenes, i.e. MuRF1 and MAFbx). In contrast to increased autophagy signalling at 7 days, while MAFbx/Atrogin-1 tended to decrease but without reaching significance ($t(8)=0.28$, $p>0.05$; Supplementary Figure 1a), MuRF1 protein content was decreased in ischemic muscle ($t(8)=3.099$, $p<0.05$; Supplementary Figure 1c). At 28 days, however, atrogene expression was normalised in line with autophagy signalling ($p>0.05$; Supplementary Figure 1d). Overall these data indicate autophagy signalling is activated at early HLI stages but with potential inhibition of proteasome–dependent catabolic activity.

Mitophagy and mitochondria

An important aspect of autophagy is mitophagy, which maintains mitochondrial quality control by recycling mitochondrial proteins to preserve metabolic reserve. Mitophagy markers including phosphorylated dynamin-like protein 1 (Drp1; a marker of mitochondrial fission) increased at 7 days HLI ($U(8)= -1.72$, $p<0.05$; Figure 4a) despite no difference between groups for optic atrophy 1 protein (OPA-1- $p>0.05$; Figure 4c) and Mitofusin 2 (Mfn2 - $p>0.05$; Figure 4e) two markers of mitochondria fusion. After 28 days, both Drp1, OPA1 and Mfn2 were not different between conditions ($p>0.05$, Figure 4b, d, f). Given these early changes in mitophagy markers, we next measured citrate synthase activity in order to provide an index of mitochondrial content. Citrate synthase activity was decreased at 7 days HLI ($t(8)=4.568$, $p<0.05$; Figure 4f) and remained reduced at 28 days compared to contralateral muscle ($t(4.4)=3.27$, $p<0.05$; Figure 4g), which indicates an early and sustained loss of muscle mitochondrial content in HLI muscles.

Temporal-dependent changes in Sestrins may regulate autophagy in HLI

Given our findings indicated that early muscle loss in HLI is associated with robust autophagy signalling alongside apparent inhibition of proteasome signalling, we next explored upstream regulators of autophagy. We first investigated whether the expression of the Sestrins family, known to influence autophagy-dependent muscle

309 remodelling, was altered in HLI. Protein content of Sestrin 1 tended to decreased by
310 1-fold 7 days following HLI vs. contralateral control muscle ($t(4.2)=3.832$, $p<0.05$;
311 Figure 5a). This was in contrast to Sestrin 2, where protein expression increased by
312 2-fold ($t(4.3)=-4.281$, $p<0.05$. Figure 5c). After 28 days HLI, both Sestrin 1 and
313 Sestrin 2 expression were normalised to control values ($p>0.05$; Figure 5b, d).
314 Together, these findings suggest that a complex interplay exists between Sestrin 1
315 and 2 expression that could impact autophagy signalling during muscle remodelling
316 in HLI. As Sestrins regulate autophagy (and UPS) by modulating AMP-activated
317 protein kinase (AMPK) which phosphorylation increased in HLI at 7 days ($t(5)=-$
318 3.755, $p<0.05$; Figure 5e) but normalised to control levels in HLI 28 days ($p>0.05$;
319 Figure 6f).
320
321 Sestrins have inherent antioxidant properties and also regulate redox homeostasis
322 via Nrf2. As muscle biopsies from HLI patients show oxidative damage (4), we next
323 assessed antioxidant expression profile. At 7 days post HLI, expression of the mainly
324 cytosolic antioxidant superoxide dismutase 1 (CuZnSOD) was decreased
325 ($t(8)=3.827$, $p<0.05$; Figure 5g) while the mitochondrial isoform belonging to the
326 same family, superoxide dismutase 2 (MnSOD) tended to be reduced but without
327 reaching significance ($t(5.09)=1.569$, $p=0.177$; Figure 5i). However, at 28 days
328 antioxidant expression was normalised to control and no differences observed in
329 CuZnSOD or MnSOD following HLI ($p>0.05$; Figure 5h, l). Furthermore, we did not
330 detect differences in the content of Heme Oxygenase 1 at both 7 and 28 days (HO-1
331 - $p>0.05$, Supplementary figure 1e, f), a Nrf2 regulated enzyme that offers oxidative
332 and inflammatory protection. Overall, these data suggest HLI perturbs Sestrin
333 signalling in line with autophagy activation and an overall downregulated antioxidant
334 expression.
335
336 **Markers for anabolic signalling were unchanged in HLI**
337 Given the recovery of muscle mass and cross-sectional area seen in the late-HLI
338 group, we investigated whether HLI was affecting regulation of protein synthesis in
339 skeletal muscle by measuring two key readouts in the mTORC1 signalling pathway.
340 Phosphorylation levels eukaryotic translation initiation factor 4E-binding protein 1
341 (4EBP1) and ribosomal protein S6 (rbS6) remained unchanged in ischemic vs.
342 contralateral muscle both at 7 and 28 days ($p>0.05$; Figure 6a-d).

343

344

345

Discussion

Our understanding of the mechanisms that cause muscle-related disability in patients with HLI remains partially resolved. In the present study, by investigating a temporal experimental model of HLI, we showed that muscle wasting occurred at early-stage (7 days) but was fully normalised within weeks at late-stage (28 days). Early-onset muscle wasting was closely mirrored by a robust increase in markers of catabolic-autophagy signalling. Early and sustained loss of mitochondria content in HLI was closely associated with dysregulated expression of mitophagy proteins. Our data indicate HLI may modulate the sestrin-autophagy signalling axis to drive loss of muscle mass, given sestrin 2 was upregulated early in parallel to reduced antioxidant enzyme expression. Surprisingly, a divergent pattern for sestrin 1 expression was found, which raises the question of whether cross-talk or redundancy exists in sestrins following HLI to impact muscle mass.

Muscle atrophy is associated with activated autophagy in HLI

Patients with HLI experience changes to muscle homeostasis that cause severe muscle wasting and disability (1, 4, 7, 23, 35, 36). A lack of consensus on the mechanisms responsible exist however, in particular regarding the role of autophagy. In the present study, 7 days following HLI we reported a decreased blood flow compared to the control limb (>70%) which translated to reductions in muscle mass (both GC and soleus). This muscle wasting is attributed to a 20% reduction in overall fibre CSA and an absolute loss of Type I fibres following HLI, with recent suggestions that hypoxia (both environmental and pathological) may underlie such changes (37). Several different pathways are known to drive skeletal muscle atrophy and in particular the UPS and autophagy (38). The UPS is upregulated in several conditions characterised by muscle wasting (38) with MuRF1 and Atrogin-1 shown to play a pivotal role in this pathway. Our analysis showed that in ischemic muscle MuRF1 and Atrogin-1 expression is decreased when compared to the contralateral leg suggesting that during ischemia the muscle wasting in HLI may not be driven exclusively by the UPS but rather by alternative pathways. However, it is worth mentioning that a previous study (39) reported hyperactivation of these enzymes at early stages post-HLI suggesting that, while the UPS may play an important role in the immediate aftermath of the ischemic injury, in the long-term its role may become secondary.

Several different pathways drive muscle atrophy, including autophagy (8). Autophagy is an important pathway allowing maintenance of cellular homeostasis but when dysregulated triggers muscle wasting (40, 41). Our data suggest that HLI causes early increases in muscle Beclin-1, LC3-I and LC3-II protein content. These proteins play an important role in regulating autophagosome induction and maturation and are considered reliable markers of autophagy (42). We also found a decrease in the protein expression of p62, a cargo protein responsible for delivering dysfunctional proteins and organelles to the autolysosome for degradation being degraded itself in the process (10). Cellular content of p62 protein content is inversely correlated to autophagy (43), therefore low p62 expression reinforces our hypothesis that autophagy is upregulated in HLI and serves as a key trigger for early-onset muscle wasting. Autophagy acts to maintain a healthy pool of mitochondria in a process known as mitophagy which can become unbalanced, thus eliminating damaged and dysfunctional mitochondria and forgoing quantity over quality (11). This is particularly relevant in HLI where muscle biopsies from patients have reduced mitochondrial number (4). At 7 days post HLI, our data confirmed loss of mitochondria content in line with disturbed mitophagy (i.e. increased fission), as evidenced by elevated Drp1 phosphorylation (44) despite no change to markers of fusion. Mitochondria loss was sustained at 28 days following HLI, despite mitophagy markers and muscle size recovering. A disconnection between muscle mass/function and mitochondria activity does not seem to be uncommon in HLI, with a recent patient study showing that, in response to exercise, improved muscle function and fibre CSA were not associated with changes in mitochondria number and activity [45]. The meaning behind the lack of recovery in mitochondrial properties compared to muscle mass remains unexplored in ischemic conditions and further studies are warranted. For example, this lag in recovery of muscle mitochondria compared to mass may explain prolonged fatigue-related symptoms experienced by HLI patients.

Molecular regulators of autophagy in HLI via AMPK and Sestrins

Several proteins are involved in maintaining a tight balance between cellular anabolism and catabolism, and specifically autophagy regulation. Among these, mTORC1 plays a pivotal role in orchestrating anabolic and catabolic responses to environmental changes including autophagy inhibition (45) (46). No changes in reliable mTORC1 downstream signalling markers (4EBP1 and rbS6) were found post

HLI and, despite being unable to exclude that the mTORC1 axis remains unaffected during HLI, further studies are warranted to determine levels of mTORC1 activation in HLI. To further investigate other molecular regulars of autophagy, we found phosphorylation levels of AMPK were increased following HLI at 7 days. Once phosphorylated, AMPK, a central energy sensor regulating cellular metabolism and energy homeostasis, promotes autophagy and mitophagy via several pathways. Specifically, it is known that AMPK can promote autophagy directly through the phosphorylation of specific targets in the mTOCR1, ULK1 and PIK3C3/VPS34 complexes but also by regulating transcription factors such as FOXO3, Transcription factor EB and Bromodomain-containing protein 4 (47). Overall, our data suggest that upon induction of HLI, AMPK-dependent autophagy activation likely serves to accelerate muscle remodelling that exacerbate early muscle loss. Further studies are warranted to determine the specific pathway of AMPK-autophagy activation in early HLI.

Sestrins are regarded to be critical for maintenance of skeletal muscle homeostasis (20). Sestrins control autophagy to promote proteostasis that preserves muscle mass and function (18). We found Sestrin 1 content decreased but Sestrin 2 increased early following HLI. Is reduced Sestrin 1 content a compensatory response to elevated Sestrin 2 levels? Past studies have shown that in sarcopenic muscle, Sestrin 1 expression tends to decrease similar to our data in HLI (20). In contrast to Sestrin 1, Sestrin 2 is activated under hypoxic conditions induced by ischemic injury as most widely characterised in myocardial ischemia/reperfusion injury (48). Lower oxygen perfusion to ischemic muscle (15, 49, 50) may promote Sestrin 2 activation (28). Sestrin 2 regulates skeletal muscle homeostasis (48), which includes playing a pivotal role in autophagy regulation via AMPK signalling (51). It has been previously reported that Sestrin 2 can induce AMPK phosphorylation via the Serine/threonin kinase 11 to promote autophagy activation (48). By phosphorylating AMPK, Sestrin 2 appears to be a central regulator of the autophagic response following HLI. While this may initially contribute to the wasting process, it may also be essential for supporting long-term muscle muss survival and regeneration (16, 52). For example, administration to ischemic mice of the autophagy inhibitor chloroquine reduced muscle function and regenerating potential of myocytes, despite initially conferring protection against muscle wasting (16, 52). Our data support this hypothesis, as 28

448 days following HLI we found a recovery of muscle mass that was associated with
449 normalised fibre CSA, reappearance of type I fibres, and appearance of centralised
450 nuclei (i.e. a marker of fibre regeneration that is commonly observed during skeletal
451 muscle repair following injury (53, 54)). The progressive improvement of the skeletal
452 muscle morphology, together with the metabolic changes reported, suggest that
453 despite the initial response to HLI causing early-onset muscle wasting, this may be
454 an important physiological response regulated by Sestrin 2 and AMPK that overall
455 aims to protect muscle survival and enhance recovery under the most extreme
456 stresses.
457
458 Another important role Sestrins may play in skeletal muscle is as antioxidants (i.e
459 directly or via regulating the NRF2 antioxidant signalling pathway) (20). While the
460 intrinsic catalytic activity of Sestrin 2 as an antioxidant remains unclear (48), there is
461 evidence to suggest it promotes transcription of specific antioxidant genes including
462 superoxide dismutase and Heme-oxygenase 1 (48). Due to limited tissue availability,
463 we were only able to measure the protein content of some antioxidant enzymes and
464 future studies aimed to further explore the interaction between sestrins and the
465 NRF2 antioxidant system in HLI are warranted. Our data showed that the protein
466 content of the antioxidant enzymes CuZnSOD and MnSOD were decreased in HLI
467 compared to control while HO-1 remain unchanged (Supplementary figure 1), which
468 aligns with other atrophic conditions characterised by oxidative stress (43, 48) and
469 that was reported by a previous study in HLI C57Bl/6 female mice (55).
470
471 **Conclusions**
472 In conclusion, we have shown that HLI triggers robust remodelling in skeletal muscle
473 structure including early-onset muscle atrophy loss at 7 days that is normalised later
474 at 28 days. Early muscle wasting following HLI muscles was associated with
475 activated catabolic-autophagy signalling, which was closely linked to Sestrin2-AMPK
476 signalling. Sestrins could act as potential upstream regulators of autophagy-
477 dependent early muscle loss following HLI.
478
479 **Acknowledgments**
480 The authors would also like to thank Natallia Makova and Anna Skromna for their
481 excellent assistance supporting Laser Doppler measurements and Dr Diana Renteria

Ramirez for her assistance in samples preparation. This work was supported by MRC UK (MR/S025472/1) and Defence And Security Accelerator (DASA - ACC2011654). The authors declare no conflict of interest.

Figures legend

Figure 1. Representative images of blood flow in the lower hind limbs before (Pre-Op), 7 Days and 28 Days after surgery (**a**). At 7 days post-HLI, blood flow (red/yellow) was significantly reduced in ischemic leg (-73%, $p<0.001$ - **b**) compared to contralateral limb. However, at 28 days post-ischemia, the blood flow was partially restored (-44%, $p>0.05$ - **c**) as a result of femoral artery collateralization. No differences in total body weight were seen 7 days post-HLI ($p>0.05$ - **d**) while a significant increase was seen in total body weight after surgery at 28 days ($p<0.05$ - **e**). Muscle wet weight was significantly decreased in the GC ($p<0.01$ - **f**) and soleus ($p<0.05$ - **h**) 7 days post-HLI but recovered at 28 days in both GC (**g**) and Soleus (**i**). Histograms represent the mean and the standard error of the mean for each experimental group (n=10). * $p<0.05$ - ** $p<0.01$ - *** $p<0.001$ compared with the control group.

Figure 2. Representative images of sections from non-ischemic (control) and 7 days post-HLI soleus muscle stained for MyHC isoforms (Type I - red, Type IIa - green, Type IIb/x - black, fibre boundaries - blue) (**a, d**). At 7 days post-HLI there is a significant reduction of fibre CSA (n=8, $p<0.01$ - **b**) with an absolute loss of type I fibres (n=8, -20%, $p<0.01$ - **c**) compared to contralateral limb. In line with the recovery of muscle mass seen at 28 days post-HLI, CSA is recovered with no differences compared to the contralateral limb (n=10, $p>0.05$ - **e**) and with reappearance of type I fibres (n=8, $p>0.05$ - **f**). A robust regenerative potential at 28 days was confirmed by a significant increase in fibres with centralised nuclei in the ischemic muscle compared to contralateral (n=10, +68 - $p<0.01$ - **g, h**). Histograms represent the mean and the standard error of the mean for each experimental group. * $p<0.05$ - ** $p<0.01$ - *** $p<0.001$ compared with the control group.

Figure 3. Several markers of autophagy were investigated in the gastrocnemius muscle. Beclin-1, a reliable marker of autophagy induction was significantly increased in the ischemic muscle 7 days post-HLI ($p<0.05$ - **a**). Similar trends were seen in both isoforms of LC3, a reliable marker of autophagosome formation ($p<0.05$ - **c, e**). Protein expression of p62, another reliable marker of autophagy which levels have been inversely correlated to autophagy activity, is instead decreased ($p<0.01$ - **g**) in ischemic muscle 7 days post-HLI reinforcing our hypothesis that autophagy is up-regulated and is responsible for the loss of muscle mass seen. At 28 days post-HLI, when there is recovery of muscle mass and

regeneration, the levels of Beclin-1 (**b**), LC3I (**d**), LC3II (**f**) and p62 (**h**) in the ischemic muscle are no different compared to the levels recorded in the contralateral limb. Representative images of blots were presented (**i**). Histograms represent the mean and the standard error of the mean for each experimental group (n=10). * p<0.05 - ** p<0.01 - *** p<0.001 compared with the control group.

Figure 4. Unregulated mitophagy was seen at 7 days post HLI with an increase of Drp1 phosphorylation (n=9, p<0.01) a marker of mitochondrial fission (**a**) while no changes in OPA1 content were observed (n=10, p>0.05 - **c**). At 28 days post-HLI the levels of Drp1 phosphorylation returned to contralateral levels (n=10, p>0.05 - **b**) with no differences seen also in the content of OPA1 (n=10, p>0.05 - **d**). At 7 days post-HLI dysregulated mitophagy resulted in a loss of mitochondria measured using the citrate synthase assay (n=10, p<0.01 - **f**) which was sustained up to 28 days post-HLI (n=10, p<0.05 - **g**) despite the normalisation of mitophagy. No differences were seen in Mfn2 content at 7 (n=8, p>0.05 - e), and 28 days (n=10, p>0.05 - f). Representative images of blots were presented (**g**). Histograms represent the mean and the standard error of the mean for each experimental group. * p<0.05 - ** p<0.01 - *** p<0.001 compared with the control group.

Figure 5. A different response was seen at 7 days post-HLI in the levels of the two subunits belonging to the Sestrin family analysed in this study. The levels of Sestrin 1 were reduced (n=10, p<0.01 - **a**) while Sestrin 2 were upregulated (n=8, p<0.01 - **c**) suggesting a possible compensatory cross-talk between the two proteins. In line with the increase of Sestrin 2 levels, the phosphorylation levels of AMPK were increased (n=8, p<0.01 - **e**). The levels of CuZnSOD were significantly decreased 7 days post-HLI (n=10, p<0.01 - **g**) with a similar trend seen in MnSOD (n=10, p>0.05 - **i**). At 28-days post-HLI, the levels of Sestrin 1 (**b**), Sestrin 2 (**d**), the phosphorylation levels of AMPK (**f**), CuZnSOD (**h**) and MnSOD (**l**) returned to contralateral levels (n=10, p>0.05). Representative images of blots were presented (**m**). Histograms represent the mean and the standard error of the mean for each experimental group. * p<0.05 - ** p<0.01 - *** p<0.001 compared with the control group.

Figure 6. The downstream readings of the mTORC1 signalling pathway 4EBP1 (**a, c**) and s6rb (**b, d**) were unchanged at 7 and 28 days post-HLI suggesting no activation of this signalling pathway. Representative images of blots were presented (e). Histograms represent the mean and the standard error of the mean for each experimental group.

Supplementary Figure 1. The levels of MuRF1 were decreased 7 days post-HLI (n=10, p<0.05 - **a**) with a similar trend seen for Atrogin-1 (n=9, p>0.05 - **c**) suggesting that the Ubiquitin Proteasome System is not apparently driving muscle remodelling at 7 days after ischemic injury . The levels of MuRF1 returned to contralateral levels 28 days post-HLI (n=10, p>0.05 - **b**) while we were unable to detect readings for Atrogin-1. No differences

were detected in the content of HO-1, an antioxidant response element activated by NRf2, both at 7 (n=10, p>0.05 - **e**) and 28 days (n=10, p>0.05 - **f)**. Representative images of blots were presented (**g**) together with a representative protein ladder used for our experiments (**h**). Histograms represent the mean and the standard error of the mean for each experimental group. * p<0.05 - ** p<0.01 - *** p<0.001 compared with the control group.

Supplementary table. List of the antibodies used for SDS-PAGE western blot analysis.

References

1. **Fowkes FGR, Rudan D, Rudan I, Aboyans V, Denenberg JO, McDermott MM, Norman PE, Sampson UKA, Williams LJ, Mensah GA, and Criqui MH**. Comparison of global estimates of prevalence and risk factors for peripheral artery disease in 2000 and 2010: a systematic review and analysis. *The Lancet* 382: 1329-1340, 2013.
2. **Nativel M, Potier L, Alexandre L, Baillet-Blanco L, Ducasse E, Velho G, Marre M, Roussel R, Rigalleau V, and Mohammedi K**. Lower extremity arterial disease in patients with diabetes: a contemporary narrative review. *Cardiovasc Diabetol* 17: 138, 2018.
3. **Weitz JI, Byrne J, Clagett GP, Farkouh ME, Porter JM, Sackett DL, Strandness DE, Jr., and Taylor LM**. Diagnosis and treatment of chronic arterial insufficiency of the lower extremities: a critical review. *Circulation* 94: 3026-3049, 1996.
4. **McDermott MM, Ferrucci L, Gonzalez-Freire M, Kosmac K, Leeuwenburgh C, Peterson CA, Saini S, and Sufit R**. Skeletal Muscle Pathology in Peripheral Artery Disease: A Brief Review. *Arterioscler Thromb Vasc Biol* 40: 2577-2585, 2020.
5. **McDermott MM, Guralnik JM, Criqui MH, Ferrucci L, Liu K, Spring B, Tian L, Domanchuk K, Kibbe M, Zhao L, Lloyd Jones D, Liao Y, Gao Y, and Rejeski WJ**. Unsupervised exercise and mobility loss in peripheral artery disease: a randomized controlled trial. *J Am Heart Assoc* 4: 2015.
6. **Hiatt WR, Regensteiner JG, Wolfel EE, Carry MR, and Brass EP**. Effect of exercise training on skeletal muscle histology and metabolism in peripheral arterial disease. *J Appl Physiol (1985)* 81: 780-788, 1996.
7. **McDermott MM**. Functional impairment in peripheral artery disease and how to improve it in 2013. *Curr Cardiol Rep* 15: 347, 2013.
8. **Scalabrin M, Adams V, Labeit S, and Bowen TS**. Emerging Strategies Targeting Catabolic Muscle Stress Relief. *Int J Mol Sci* 21: 2020.
9. **Neel BA, Lin Y, and Pessin JE**. Skeletal muscle autophagy: a new metabolic regulator. *Trends Endocrinol Metab* 24: 635-643, 2013.
10. **Rusten TE, and Stenmark H**. p62, an autophagy hero or culprit? *Nat Cell Biol* 12: 207-209, 2010.
11. **Ji LL, and Yeo D**. Mitochondrial dysregulation and muscle disuse atrophy. *F1000Res* 8: 2019.
12. **Desgeorges MM, Devillard X, Toutain J, Divoux D, Castells J, Bernaudin M, Touzani O, and Freyssenet DG**. Molecular mechanisms of skeletal muscle atrophy in a mouse model of cerebral ischemia. *Stroke* 46: 1673-1680, 2015.
13. **Liu C, Peng M, Zheng L, Zhao Y, Wang R, Su Q, Chen S, and Li Z**. Enhanced autophagy alleviates injury during hindlimb ischemia/reperfusion in mice. *Exp Ther Med* 18: 1669-1676, 2019.
14. **Albadawi H, Oklu R, Milner JD, Uong TP, Yoo HJ, Austen WG, Jr., and Watkins MT**. Effect of limb demand ischemia on autophagy and morphology in mice. *J Surg Res* 198: 515-524, 2015.
15. **Jeong IH, Bae WY, Choi JS, and Jeong JW**. Ischemia induces autophagy of endothelial cells and stimulates angiogenic effects in a hindlimb ischemia mouse model. *Cell Death Dis* 11: 624, 2020.

16. **Sachdev U, Ferrari R, Cui X, Pius A, Sahu A, Reynolds M, Liao H, Sun P, Shinde S, Ambrosio F, Shiva S, Loughran P, and Scott M**. Caspase1/11 signaling affects muscle regeneration and recovery following ischemia, and can be modulated by chloroquine. *Mol Med* 26: 69, 2020.
17. **He C, and Klionsky DJ**. Regulation mechanisms and signaling pathways of autophagy. *Annu Rev Genet* 43: 67-93, 2009.
18. **Segales J, Perdiguero E, Serrano AL, Sousa-Victor P, Ortet L, Jardi M, Budanov AV, Garcia-Prat L, Sandri M, Thomson DM, Karin M, Hee Lee J, and Munoz-Canoves P**. Sestrin prevents atrophy of disused and aging muscles by integrating anabolic and catabolic signals. *Nat Commun* 11: 189, 2020.
19. **Pasha M, Eid AH, Eid AA, Gorin Y, and Munusamy S**. Sestrin2 as a Novel Biomarker and Therapeutic Target for Various Diseases. *Oxid Med Cell Longev* 2017: 3296294, 2017.
20. **Kim M, Sujkowski A, Namkoong S, Gu B, Cobb T, Kim B, Kowalsky AH, Cho CS, Semple I, Ro SH, Davis C, Brooks SV, Karin M, Wessells RJ, and Lee JH**. Sestrins are evolutionarily conserved mediators of exercise benefits. *Nat Commun* 11: 190, 2020.
21. **Yang BA, Castor-Macias J, Fraczek P, Cornett A, Brown LA, Kim M, Brooks SV, Lombaert IMA, Lee JH, and Aguilar CA**. Sestrins regulate muscle stem cell metabolic homeostasis. *Stem Cell Reports* 16: 2078-2088, 2021.
22. **Rhee SG, and Bae SH**. The antioxidant function of sestrins is mediated by promotion of autophagic degradation of Keap1 and Nrf2 activation and by inhibition of mTORC1. *Free Radic Biol Med* 88: 205-211, 2015.
23. **Hourde C, Vignaud A, Beurdy I, Martelly I, Keller A, and Ferry A**. Sustained peripheral arterial insufficiency durably impairs normal and regenerating skeletal muscle function. *J Physiol Sci* 56: 361-367, 2006.
24. **Mohiuddin M, Lee NH, Moon JY, Han WM, Anderson SE, Choi JJ, Shin E, Nakhai SA, Tran T, Aliya B, Kim DY, Gerold A, Hansen LM, Taylor WR, and Jang YC**. Critical Limb Ischemia Induces Remodeling of Skeletal Muscle Motor Unit, Myonuclear-, and Mitochondrial-Domains. *Sci Rep* 9: 9551, 2019.
25. **Paek R, Chang DS, Brevetti LS, Rollins MD, Brady S, Ursell PC, Hunt TK, Sarkar R, and Messina LM**. Correlation of a simple direct measurement of muscle pO(2) to a clinical ischemia index and histology in a rat model of chronic severe hindlimb ischemia. *J Vasc Surg* 36: 172-179, 2002.
26. **Tang GL, Chang DS, Sarkar R, Wang R, and Messina LM**. The effect of gradual or acute arterial occlusion on skeletal muscle blood flow, arteriogenesis, and inflammation in rat hindlimb ischemia. *J Vasc Surg* 41: 312-320, 2005.
27. **Hsieh PL, Rybalko V, Baker AB, Suggs LJ, and Farrar RP**. Recruitment and therapeutic application of macrophages in skeletal muscles after hind limb ischemia. *J Vasc Surg* 67: 1908-1920 e1901, 2018.
28. **Lee CW, Stabile E, Kinnaird T, Shou M, Devaney JM, Epstein SE, and Burnett MS**. Temporal patterns of gene expression after acute hindlimb ischemia in mice: insights into the genomic program for collateral vessel development. *J Am Coll Cardiol* 43: 474-482, 2004.
29. **Paoni NF, Peale F, Wang F, Errett-Baroncini C, Steinmetz H, Toy K, Bai W, Williams PM, Bunting S, Gerritsen ME, and Powell-Braxton L**. Time course of skeletal muscle repair and gene expression following acute hind limb ischemia in mice. *Physiol Genomics* 11: 263-272, 2002.
30. **Scalabrin M, Pollock N, Staunton CA, Brooks SV, McArdle A, Jackson MJ, and Vasilaki A**. Redox responses in skeletal muscle following denervation. *Redox Biol* 26: 101294, 2019.
31. **Espino-Gonzalez E, Tickle PG, Benson AP, Kissane RWP, Askew GN, Egginton S, and Bowen TS**. Abnormal skeletal muscle blood flow, contractile mechanics and fibre morphology in a rat model of obese-HFpEF. *J Physiol* 599: 981-1001, 2021.
32. **Whitehead A, Krause FN, Moran A, MacCannell ADV, Scragg JL, McNally BD, Boateng E, Murfitt SA, Virtue S, Wright J, Garnham J, Davies GR, Dodgson J, Schneider JE, Murray AJ, Church C, Vidal-Puig A, Witte KK, Griffin JL, and Roberts LD**. Brown and beige adipose tissue regulate systemic metabolism through a metabolite interorgan signaling axis. *Nat Commun* 12: 1905, 2021.

33. **Motulsky HJ, and Brown RE**. Detecting outliers when fitting data with nonlinear regression - a new method based on robust nonlinear regression and the false discovery rate. *BMC Bioinformatics* 7: 123, 2006.
34. **Meyer G, Czompa A, Reboul C, Csepanyi E, Czegledi A, Bak I, Balla G, Balla J, Tosaki A, and Lekli I**. The cellular autophagy markers Beclin-1 and LC3B-II are increased during reperfusion in fibrillated mouse hearts. *Curr Pharm Des* 19: 6912-6918, 2013.
35. **Goldberg EJ, Schmidt CA, Green TD, Karnekar R, Yamaguchi DJ, Spangenberg EE, and McClung JM**. Temporal Association Between Ischemic Muscle Perfusion Recovery and the Restoration of Muscle Contractile Function After Hindlimb Ischemia. *Front Physiol* 10: 804, 2019.
36. **Hoinoiu B, Jiga LP, Nistor A, Dornean V, Barac S, Miclaus G, Ionac M, and Hoinoiu T**. Chronic Hindlimb Ischemia Assessment; Quantitative Evaluation Using Laser Doppler in a Rodent Model of Surgically Induced Peripheral Arterial Occlusion. *Diagnostics (Basel)* 9: 2019.
37. **Lemieux P, and Birot O**. Altitude, Exercise, and Skeletal Muscle Angio-Adaptive Responses to Hypoxia: A Complex Story. *Front Physiol* 12: 735557, 2021.
38. **Sandri M**. Protein breakdown in muscle wasting: role of autophagy-lysosome and ubiquitin-proteasome. *Int J Biochem Cell Biol* 45: 2121-2129, 2013.
39. **McClung JM, McCord TJ, Keum S, Johnson S, Annex BH, Marchuk DA, and Kontos CD**. Skeletal muscle-specific genetic determinants contribute to the differential strain-dependent effects of hindlimb ischemia in mice. *Am J Pathol* 180: 2156-2169, 2012.
40. **Aman Y, Schmauck-Medina T, Hansen M, Morimoto RI, Simon AK, Bjedov I, Palikaras K, Simonsen A, Johansen T, Tavernarakis N, Rubinsztein DC, Partridge L, Kroemer G, Labbadia J, and Fang EF**. Autophagy in healthy aging and disease. *Nature Aging* 1: 634-650, 2021.
41. **Chun Y, and Kim J**. Autophagy: An Essential Degradation Program for Cellular Homeostasis and Life. *Cells* 7: 2018.
42. **Gomez-Sanchez R, Yakhine-Diop SM, Rodriguez-Arribas M, Bravo-San Pedro JM, Martinez-Chacon G, Uribe-Carretero E, Pinheiro de Castro DC, Pizarro-Estrella E, Fuentes JM, and Gonzalez-Polo RA**. mRNA and protein dataset of autophagy markers (LC3 and p62) in several cell lines. *Data Brief* 7: 641-647, 2016.
43. **Komatsu M, Waguri S, Koike M, Sou YS, Ueno T, Hara T, Mizushima N, Iwata J, Ezaki J, Murata S, Hamazaki J, Nishito Y, Iemura S, Natsume T, Yanagawa T, Uwayama J, Warabi E, Yoshida H, Ishii T, Kobayashi A, Yamamoto M, Yue Z, Uchiyama Y, Kominami E, and Tanaka K**. Homeostatic levels of p62 control cytoplasmic inclusion body formation in autophagy-deficient mice. *Cell* 131: 1149-1163, 2007.
44. **Mishra P, and Chan DC**. Metabolic regulation of mitochondrial dynamics. *J Cell Biol* 212: 379-387, 2016.
45. **Dunlop EA, and Tee AR**. mTOR and autophagy: a dynamic relationship governed by nutrients and energy. *Semin Cell Dev Biol* 36: 121-129, 2014.
46. **Rabanal-Ruiz Y, Otten EG, and Korolchuk VI**. mTORC1 as the main gateway to autophagy. *Essays Biochem* 61: 565-584, 2017.
47. **Li Y, and Chen Y**. AMPK and Autophagy. *Adv Exp Med Biol* 1206: 85-108, 2019.
48. **Gong L, Wang Z, Wang Z, and Zhang Z**. Sestrin2 as a Potential Target for Regulating Metabolic-Related Diseases. *Front Endocrinol (Lausanne)* 12: 751020, 2021.
49. **Bajwa A, Wesolowski R, Patel A, Saha P, Ludwinski F, Smith A, Nagel E, and Modarai B**. Assessment of tissue perfusion in the lower limb: current methods and techniques under development. *Circ Cardiovasc Imaging* 7: 836-843, 2014.
50. **Monteiro Rodrigues L, Silva H, Ferreira H, Renault MA, and Gadeau AP**. Observations on the perfusion recovery of regenerative angiogenesis in an ischemic limb model under hyperoxia. *Physiol Rep* 6: e13736, 2018.
51. **Kim J, Lim YM, and Lee MS**. The Role of Autophagy in Systemic Metabolism and Human-Type Diabetes. *Mol Cells* 41: 11-17, 2018.

701 52. **Lin XL, Xiao WJ, Xiao LL, and Liu MH**. Molecular mechanisms of autophagy in cardiac
702 ischemia/reperfusion injury (Review). *Mol Med Rep* 18: 675-683, 2018.
703 53. **Folker ES, and Baylies MK**. Nuclear positioning in muscle development and disease. *Front*
704 *Physiol* 4: 363, 2013.
705 54. **Roman W, and Gomes ER**. Nuclear positioning in skeletal muscle. *Semin Cell Dev Biol* 82: 51-
706 56, 2018.
707 55. **Pipinos, II, Swanson SA, Zhu Z, Nella AA, Weiss DJ, Gutti TL, McComb RD, Baxter BT, Lynch**
708 **TG, and Casale GP**. Chronically ischemic mouse skeletal muscle exhibits myopathy in association
709 with mitochondrial dysfunction and oxidative damage. *Am J Physiol Regul Integr Comp Physiol* 295:
710 R290-296, 2008.

711

Skeletal muscle remodelling post hindlimb ischemia

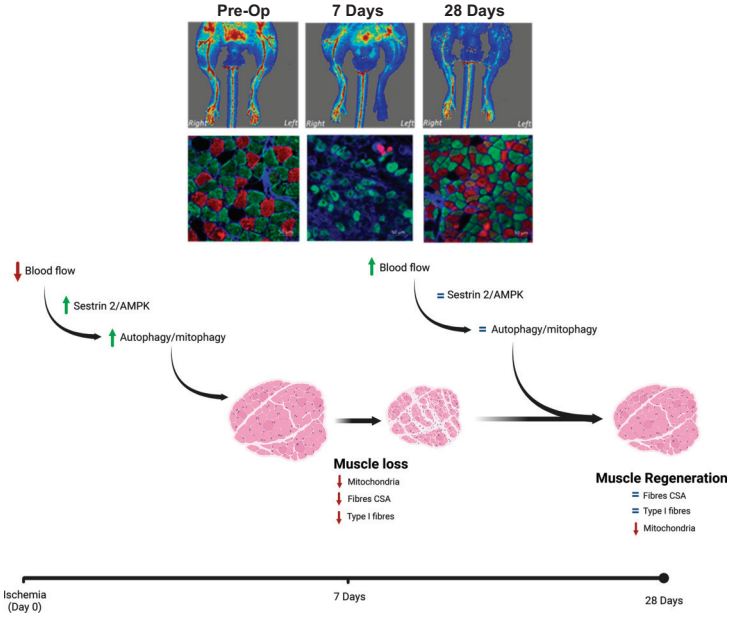

A complex interplay between Sestrins-AMPK to regulate autophagy signalling in early-to-late hindlimb ischemia appears to be central for muscle remodelling.

AMERICAN JOURNAL OF PHYSIOLOGY
CELL PHYSIOLOGY

american physiological society

Figure 1

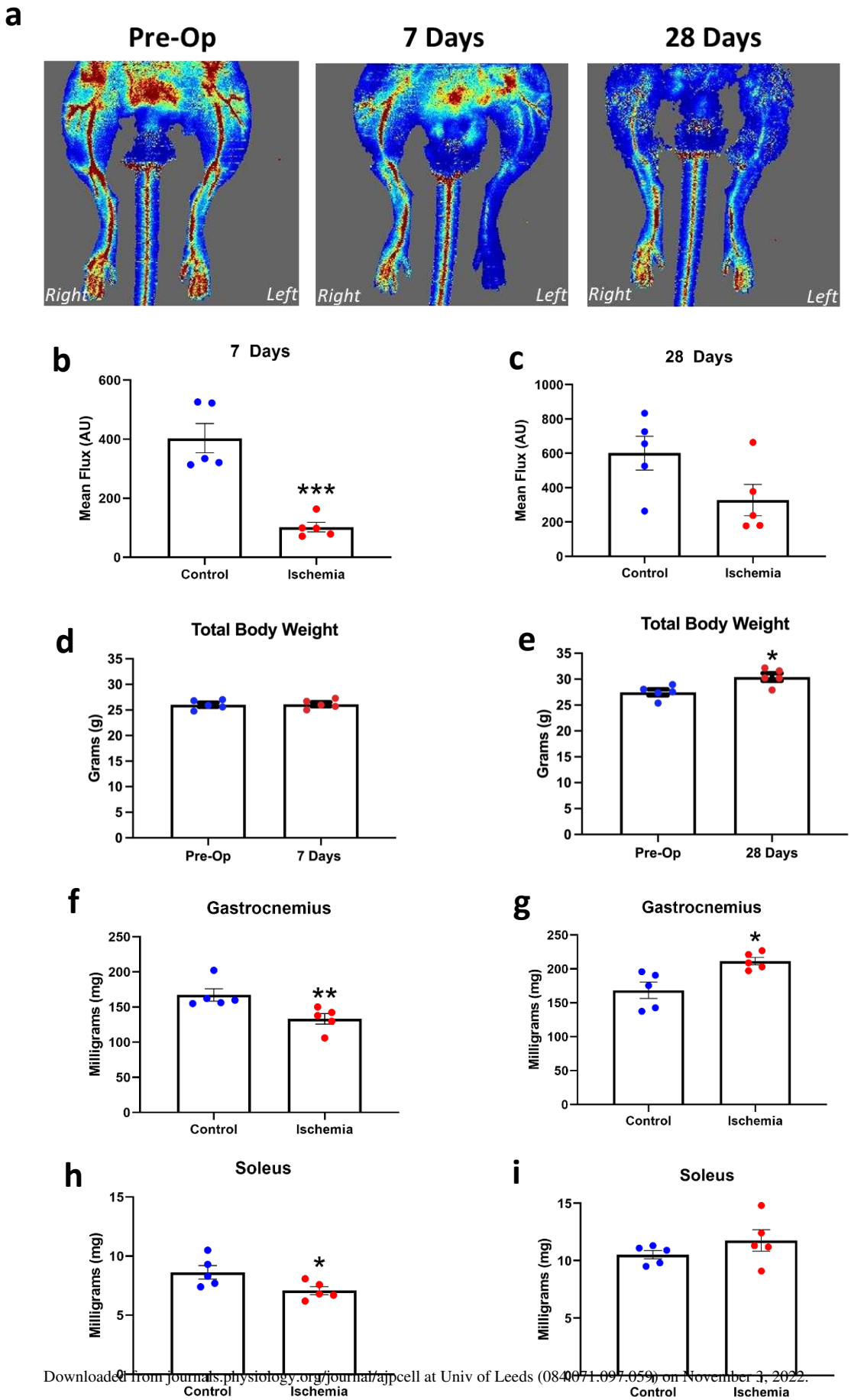

Figure 2

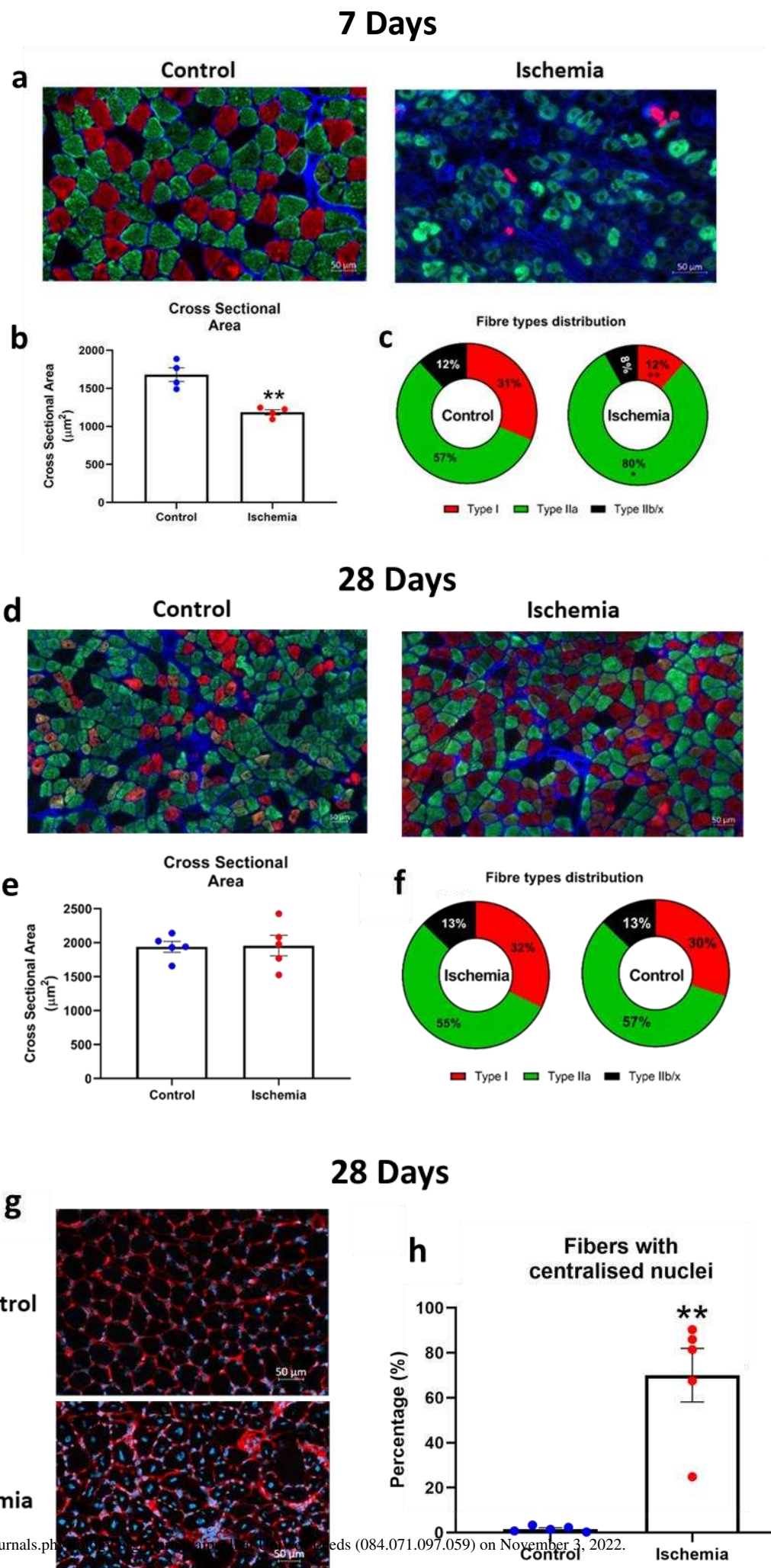

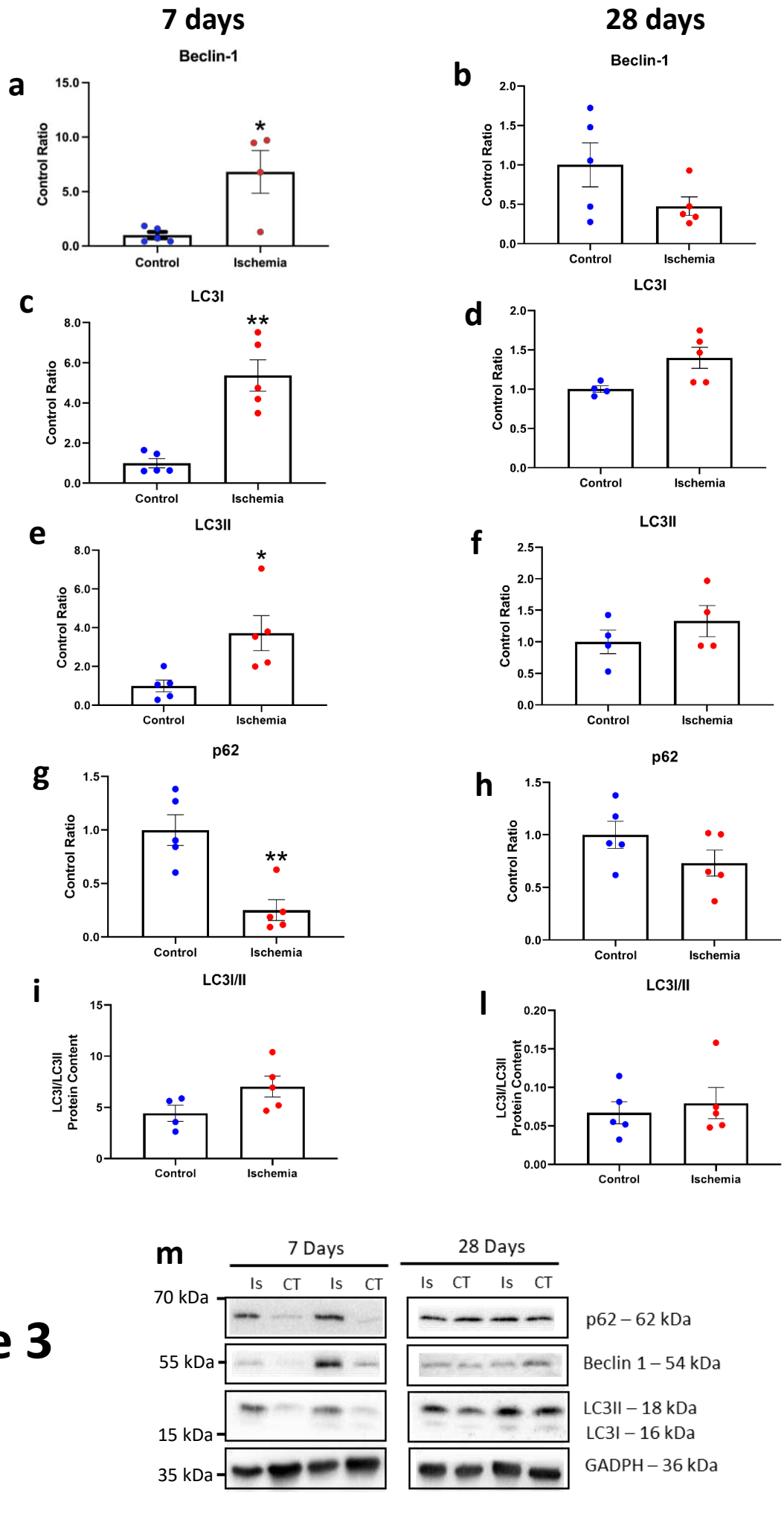

Figure 3

Figure 4

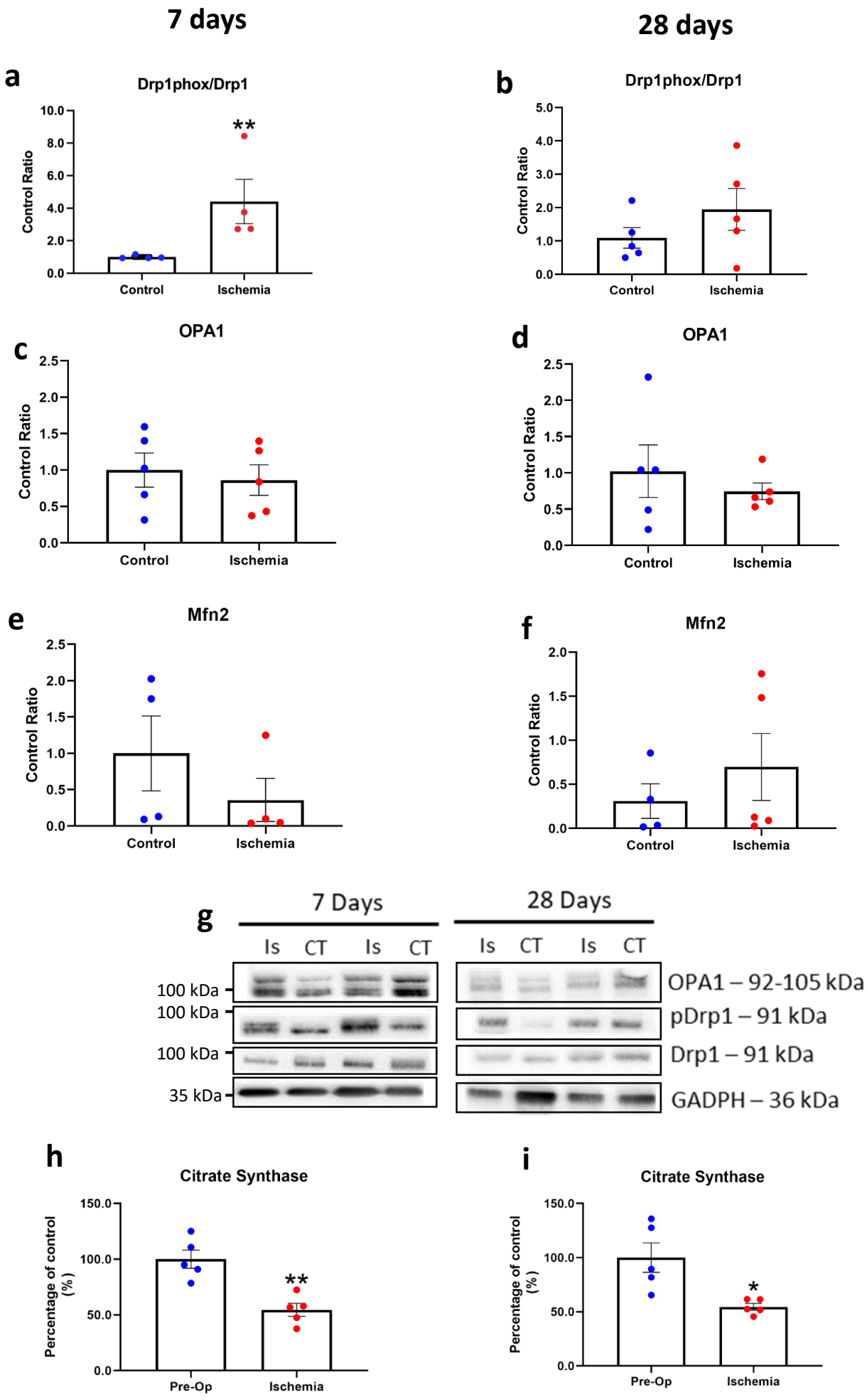

Figure 5

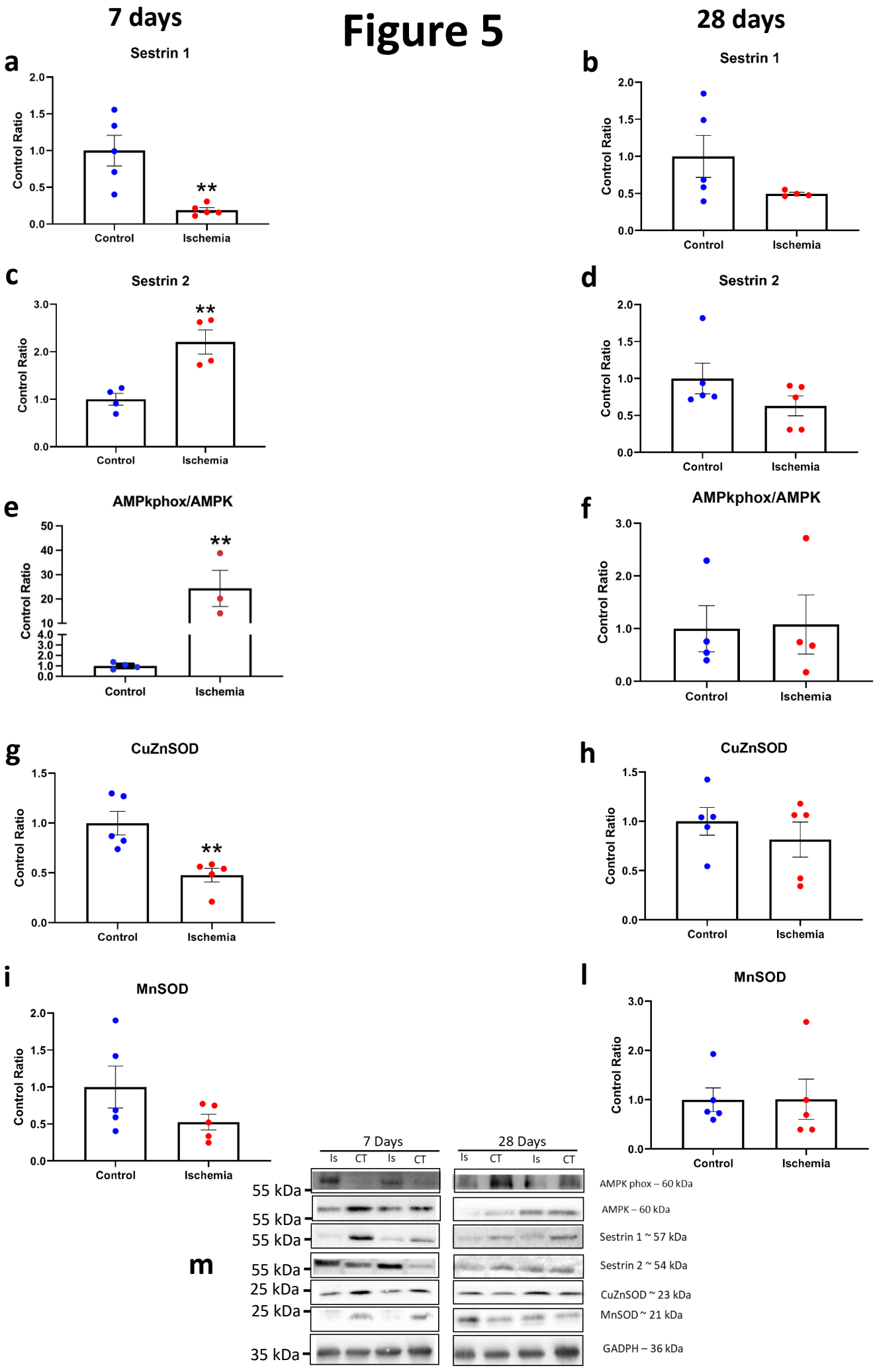

Figure 6